Out-of-Time-Ordered-Correlator Quasiprobabilities Robustly Witness Scrambling

José Raúl González Alonso,[1,*] Nicole Yunger Halpern,[2] and Justin Dressel[1,3]
[1]Schmid College of Science and Technology, Chapman University, Orange, California 92866, USA
[2]Institute for Quantum Information and Matter, Caltech, Pasadena, California 91125, USA
[3]Institute for Quantum Studies, Chapman University, Orange, California 92866, USA

(Received 23 June 2018; published 1 February 2019)

Out-of-time-ordered correlators (OTOCs) have received considerable recent attention as qualitative witnesses of information scrambling in many-body quantum systems. Theoretical discussions of OTOCs typically focus on closed systems, raising the question of their suitability as scrambling witnesses in realistic open systems. We demonstrate empirically that the nonclassical negativity of the quasiprobability distribution (QPD) behind the OTOC is a more sensitive witness for scrambling than the OTOC itself. Nonclassical features of the QPD evolve with timescales that are robust with respect to decoherence and are immune to false positives caused by decoherence. To reach this conclusion, we numerically simulate spin-chain dynamics and three measurement protocols (the interferometric, quantum-clock, and weak-measurement schemes) for measuring OTOCs. We target experiments based on quantum-computing hardware such as superconducting qubits and trapped ions.

DOI: 10.1103/PhysRevLett.122.040404

Introduction.—Quantum many-body dynamics is *scrambling* when initially localized quantum information spreads via entanglement through many degrees of freedom. Out-of-time-ordered correlators (OTOCs) have been suggested as a way to characterize scrambling across condensed-matter and high-energy contexts [1–28]. Hence, investigating how to measure OTOCs experimentally is crucial. Different OTOC-measurement protocols have been proposed [29–32], and some experimental success has been reported [33–36]. Yet the protocols' robustness in realistic, decoherent experimental settings has just started to be explored and is emerging as an active area of research [36–41].

We study decoherence's effects on OTOCs used to witness information scrambling. We find that the OTOCs' underlying quasiprobability distributions (QPDs) can more robustly identify the key time scales that distinguish scrambling. These QPDs are extended Kirkwood-Dirac QPDs [31,42–47]. They reduce to classical joint probability distributions over the eigenvalues of the OTOC operators when the operators commute. Otherwise, the QPDs become nonclassical: individual quasiprobabilities can become negative, exceed one, or become nonreal. This nonclassicality robustly distinguishes scrambling from decoherence.

We study three OTOC-measurement protocols: the (1) interferometric [30], (2) sequential-weak measurement [31,47], and (3) quantum-clock [32] protocols. Scrambling causes the OTOC to decay over a short time interval, then remain small. Information leakage can reproduce this behavior [38], since a decohered system entangles with the environment. Quantum information spreads across many degrees of freedom, but most are outside the system. We therefore propose a modification to these protocols that uses the (coarse-grained [31]) QPD behind the OTOC to distinguish between scrambling and nonscrambling dynamics despite decoherence.

Our Letter is organized as follows. We first define the OTOC and its QPD. As a concrete example suitable for simulation with qubit architectures, we consider a spin chain switchable between scrambling and integrable dynamics. Next, we introduce dephasing, modeled on current superconducting-qubit technology, and we analyze its effect on the OTOC and its QPD. We numerically simulate the spin chain for each OTOC-measurement protocol, and we compare the OTOC's degradation by decoherence. The simulations show that the QPD's negativity distinguishes scrambling dynamics despite ambiguity in the OTOC.

OTOCs and their quasiprobabilities.—Quantum information scrambling is related to the quantum butterfly effect: localized operators' supports grow under time evolution by an appropriate nonintegrable Hamiltonian. The operators come to have large commutators with most other operators—even operators localized far from the initially considered local operator. As an example, consider a Pauli operator acting on one end of a spin chain. Another Pauli operator, acting on the opposite end, probes the propagation of quantum information. If the Hamiltonian is scrambling, an increasing number of degrees of freedom must be measured to recover the initially local information. Below, we make this intuition and its relation to the OTOC more precise.

Let H denote a quantum many-body system Hamiltonian, W and V, local far-apart operators, and ρ, a density matrix. The OTOC is defined as

 © 2019 American Physical Society

$$F(t) \coloneqq \mathrm{Tr}[W^\dagger(t)V^\dagger W(t)V\rho]. \quad (1)$$

Here, $W(t) = U(t)^\dagger W U(t)$ is evolved in the Heisenberg picture with the unitary evolution operator $U(t) \coloneqq \exp(-\mathrm{i}Ht)$. Initially, W and V commute: $[W(0), V] = 0$. If W and V are unitary, then the OTOC is related to the Hermitian square of their commutator:

$$C(t) \coloneqq \left\langle \frac{[W(t),V]^\dagger}{(2i^*)} \frac{[W(t),V]}{2i} \right\rangle = \frac{1 - \mathrm{Re}F(t)}{2}. \quad (2)$$

Otherwise, the commutator's square includes nonconstant time-ordered correlators. A Hamiltonian that scrambles information tends to grow the commutator's magnitude. This growth leads to a persistent smallness of $\mathrm{Re}F(t)$. In contrast, for a nonscrambling Hamiltonian, $W(t)$ and V approximately commute after a short recurrence time, as information quickly recollects from other parts of the system. $\mathrm{Re}F(t)$ revives to close to one.

W and V decompose as $W = \sum_w w\Pi_w^W$ and $V = \sum_v v\Pi_v^V$, where Π_w^W and Π_v^V are the projectors onto the eigenspaces corresponding to the eigenvalues w and v. The eigenspaces are degenerate, since W and V are local operators and the system is large. $F(t)$ can be expressed as an average of eigenvalues [48],

$$F(t) = \sum_{v_1,w_2,v_2,w_3} v_1 w_2 v_2^* w_3^* \tilde{p}_t(v_1,w_2,v_2,w_3), \quad (3)$$

with respect to an extended Kirkwood-Dirac [42,43] (coarse-grained) quasiprobability distribution (QPD)

$$\tilde{p}_t(v_1,w_2,v_2,w_3) \coloneqq \mathrm{Tr}(\Pi_{w_3}^{W(t)}\Pi_{v_2}^V \Pi_{w_2}^{W(t)}\Pi_{v_1}^V \rho). \quad (4)$$

$\tilde{p}_t$ was denoted by $\tilde{\mathcal{A}}_\rho$ in [31].

Equation (3) implies that the QPD $\tilde{p}_t$ exhibits the OTOC's timescales. Therefore, qualitative features of OTOCs that reflect scrambling should have counterparts in $\tilde{p}_t$.

The QPD $\tilde{p}_t$ is complex and, like a classical probability distribution, normalized: $\sum_{v_1,w_2,v_2,w_3} \tilde{p}_t(v_1,w_2,v_2,w_3) = 1$. Regions where $\tilde{p}_t$ becomes negative, exceeds one, or has a nonzero imaginary part are nonclassical. We quantify these regions' magnitudes with the *total nonclassicality* of $\tilde{p}_t$:

$$\tilde{N}(t) \coloneqq \sum_{v_1,w_2,v_2,w_3} |\tilde{p}_t(v_1,w_2,v_2,w_3)| - 1. \quad (5)$$

As we will see, even in the presence of decoherence, the total nonclassicality's evolution distinguishes integrable from nonintegrable Hamiltonians. The distinction allows the QPD to signal scrambling robustly.

Spin chain.—We illustrate with a quantum Ising chain of N qubits. For ease of comparison, we use the conventions in Refs. [49–52]:

$$H = -J\sum_{i=1}^{N-1}\sigma_i^z\sigma_{i+1}^z - h\sum_{i=1}^{N}\sigma_i^z - g\sum_{i=1}^{N}\sigma_i^x. \quad (6)$$

We set $\hbar = 1$, such that energies are measured in units of J; and times, in units of $1/J$. We fix $2\pi/J = 1\ \mu$s and simulate two cases: (1) integrable case: $h/J = 0.0$, $g/J = 1.05$ and nonintegrable case: $h/J = 0.5$, $g/J = 1.05$. These values equal those in Ref. [31]. As in Ref. [31], $W = \sigma_1^z$, and $V = \sigma_N^z$ [53].

To map this Hamiltonian onto a physical qubit system, e.g., an array of transmons [54,55], we interpret the eigenstates of $-\sigma_i^x$ as a qubit's energy eigenbasis. Each qubit has an intrinsic energy splitting of $2g$ and couples capacitively to its neighbors with energy J. Unless prepared by a measurement, the qubit relaxes to a thermal state. Therefore, as an initial state, we consider a Gibbs state at a finite temperature T: $\rho_T = \mathcal{Z}^{-1}\exp(-H/T)$, with $T/J = 1$, $\mathcal{Z} = \mathrm{Tr}[(\exp(-H/T)]$, and $k_B = 1$ [56]. Each qubit has a ground-state population of ≈ 0.8. OTOCs are usually evaluated on thermal states due to holographic interest in the thermofield double state [3,4,6–10,12,13,17].

Decoherence.—We model decoherence with a Lindblad master equation $d\rho/dt = -i[H,\rho] + \sum_{i=1}^{N+n_a}\gamma_i(L_i\rho L_i^\dagger - 1/2\{L_i^\dagger L_i, \rho\})$. Here, N denotes the number of spins and n_a, the number of ancillas required for a given protocol. We choose $L_i = \sigma_i^z$ and $\gamma_i = \gamma = 1/(2T_2^*)$. The operators L_i implement single-qubit dephasing at rates γ_i (dephasing dominates the decoherence). However, this dephasing also indirectly causes amplitude mixing due to the nondiagonal terms in the Hamiltonian. The parameter T_2^* denotes the observed exponential decay constant for the qubit coherence from chip-dependent environmental fluctuations. We have chosen an optimistic $T_2^* = 130\ \mu$s, plausible for upcoming transmon hardware [57]. We interpret the Lindblad equation as an average over the stochastic phase jumps that could occur during each length-dt time step. At each time step, a density matrix ρ updates according to

$$\rho \mapsto dt\sum_i \gamma_i L_i U(t)\rho U(t)^\dagger L_i^\dagger + L_0 U(t)\rho U(t)^\dagger L_0^\dagger. \quad (7)$$

The no-phase-jump operator is $L_0 = \sqrt{\mathbb{1} - dt\sum_i \gamma_i L_i^\dagger L_i}$. This model offers simplicity and numerical stability [58].

For each OTOC-measurement protocol, we replace the ideal time evolution with Eq. (7) and assume that time reversal implements only $U(t) \leftrightarrow U^\dagger(t)$. We distinguish between the total time elapsed in the laboratory, t_L, and the time t at which the OTOC is evaluated. Each simulated reversal of t accumulates positive lab time t_L; thus, every protocol lasts for a unique t_L. To simulate decoherence's effects on the QPD, we use the weak-measurement protocol [31,47]. The other protocols can be adapted for QPD measurements [31].

Simulation results and discussion.—Figure 1 shows the real part of the OTOC, measured in the presence of

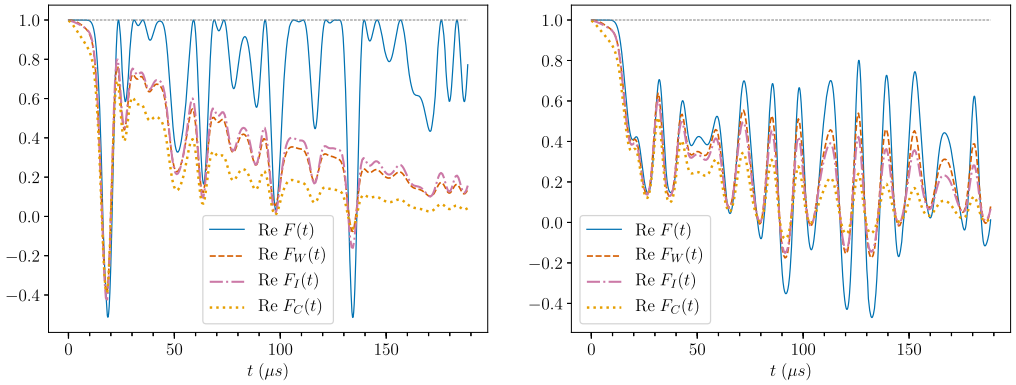

(a) Integrable case (b) Nonintegrable case

FIG. 1. Evolution of measured OTOC, $F(t) = \langle W^\dagger(t)V^\dagger W(t)V\rangle$, with and without decoherence. Values measured with three different protocols are compared against the ideal value: interferometric $F_I(t)$, weak $F_W(t)$, and quantum clock $F_C(t)$. To simulate near-term experiments, the system consists of $N = 5$ spins in an Ising chain with (a) a transverse field and (b) a transverse and a longitudinal field, with parameters detailed in the text. The system starts in a Gibbs state $\rho_T = \mathcal{Z}^{-1}\exp(-H/T)$ with $T/J = 1$ and $\mathcal{Z} = \mathrm{Tr}[\exp(-H/T)]$. The system undergoes environmental dephasing of each qubit with a decay constant of $T_2^* = 130$ μs. The local operators $W = \sigma_1^z$ and $V = \sigma_N^z$. These plots highlight the difficulties in unambiguously distinguishing between (a) nonscrambling and (b) scrambling Hamiltonians in an experimental setting with decoherence.

decoherence: $F_I(t)$, $F_W(t)$, and $F_C(t)$ denote the OTOC measured according to the interferometric [30], weak measurement [31,47], and quantum-clock [32] protocols [59]. These curves are compared to the ideal OTOC $F(t)$ measured in the absence of noise. These protocols differ in the amounts of lab time required to measure $F(t)$: the protocols need t_Ls that are at least $2t$, $3t$, and $4t$, respectively. As expected, OTOCs measured with long-t_L protocols decay the most, since they suffer from decoherence the longest. The quantum-clock protocol's $F_C(t)$ is affected the most. Nonetheless, this protocol's essence—the implementation of time reversals via an ancilla qubit—could be combined with a shorter-t_L protocol (e.g., the interferometric protocol), to mitigate decoherence [60].

Figures 1(a) and 1(b) show that decoherence hinders us from easily distinguishing between integrable and nonintegrable Hamiltonians. The integrable-Hamiltonian OTOC with decoherence decays due to information leaking, and the nonintegrable-Hamiltonian OTOC revives. If we used these two OTOCs' qualitative behaviors, we would misclassify the Hamiltonians and incur a false positive, inferring scrambling where there is none.

Distinguishing scrambling from integrable Hamiltonians via the QPD is straightforward, despite decoherence (Fig. 2). Decoherence damps the distribution's oscillations, and the different curves drift towards a common value (in our example, between 0 and 0.1). Unlike in the integrable case, the nonintegrable case's quasiprobability shows a persistent bifurcation that we call a pitchfork: around $t \approx 15$ μs quasiprobabilities that used to lie atop each at $y = 0$ split. This pitchfork arises because scrambling breaks a symmetry as it eliminates the QPD's invariance under certain permutations and negations of the QPD arguments in Eq. (4) [31]. The symmetry breaking eliminates the QPD's constancy under certain interchanges, and certain negations, of measurement outcomes in a weak-measurement trial. We should expect this asymmetry to surface in the total nonclassicality $\tilde{N}_t$ of Eq. (5). Since information scrambling is related to many-body entanglement, which is nonclassical, we expect the QPD's nonclassicality to be a robust indicator of scrambling. Indeed, damping shrinks the negative regions in Fig. 2. The negative regions also show structure that mirrors qualitative behavior of the OTOC: the decay of $\mathrm{Re}F(t)$ matches the flourishing of the negativity; the revivals of $\mathrm{Re}F(t)$ mirror the negativity's disappearance. Yet the QPD provides information absent from $F(t)$.

We plot $\tilde{N}(t)$ in Fig. 3. The nonclassicality's persistence reflects sustained noncommutativity of $W(t)$ and V. Denote by $\tilde{t}_*$ the point at which $\tilde{N}(t)$ first deviates from zero [61]; by t_m, the point at which the first maximum occurs; and by t_z, the time at which the first subsequent zero happens. For the scrambling dynamics with decoherence in Fig. 3, $t_z - t_m$ is more than an order of magnitude longer than $t_m - \tilde{t}_*$. For the nonscrambling dynamics, the two timescales are comparable. In this case, and without dissipation, $t_z - t_m$ is longer than the simulation time. We thus conjecture that, if $t_m - \tilde{t}_* \ll t_z - t_m$, the dynamics is scrambling [62]. As quantum information spreads throughout the system in a time $t_m - \tilde{t}_* \propto N$, if H is integrable, some information recollects in a time $t_z - t_m \propto N$. Hence, the total nonclassicality's first peak should be approximately symmetrical. If the system dynamics is scrambling, such a recollection would occur after a much longer time [17,63,64]. $\tilde{N}(t)$ should display strong temporal asymmetry

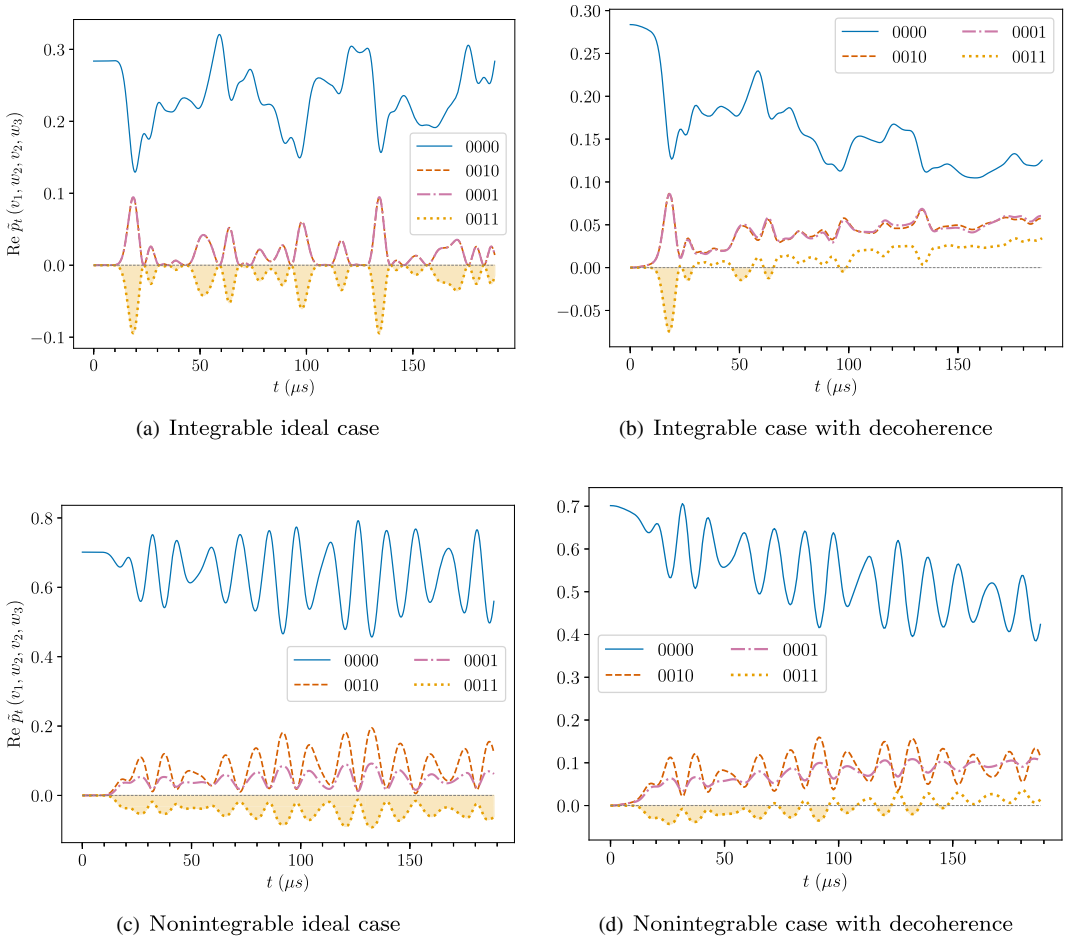

(a) Integrable ideal case

(b) Integrable case with decoherence

(c) Nonintegrable ideal case

(d) Nonintegrable case with decoherence

FIG. 2. Evolution of measured $\mathrm{Re}\tilde{p}_t$ with and without decoherence, using the sequential-weak-measurement protocol. The QPD, $\tilde{p}_t(v_1, w_2, v_2, w_3) = \mathrm{Tr}(\Pi^{W(t)}_{w_3}\Pi^{V}_{v_2}\Pi^{W(t)}_{w_2}\Pi^{V}_{v_1}\rho)$, underlies the OTOC, $F(t) = \sum v_1 w_2 v_2^* w_3^* \tilde{p}_t(v_1, w_2, v_2, w_3)$, where $V = \sum v\Pi_v$ and $W = \sum w\Pi_w$. Of the 16 QPD values, four examples are shown. The numeric labels in the legend have the form $abcd$, where $v_1 = (-1)^a$, $w_2 = (-1)^b$, $v_2 = (-1)^c$, and $w_3 = (-1)^d$. The shaded regions show nonclassical behavior of the QPD.

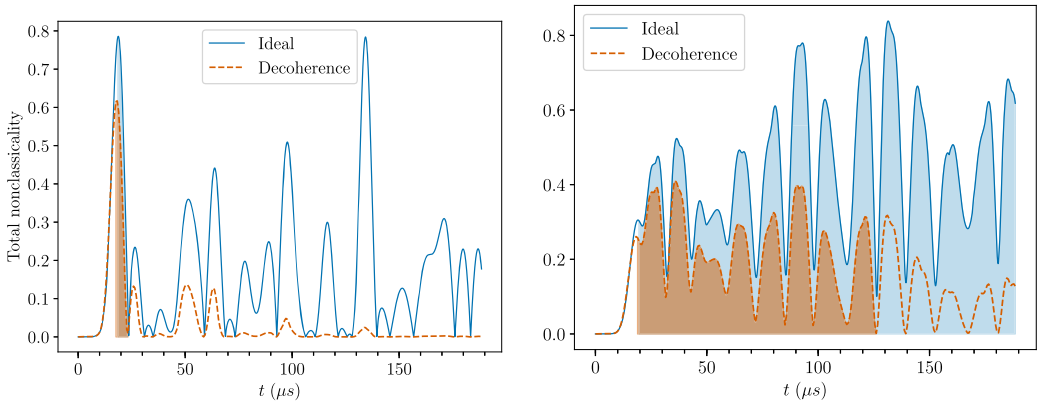

(a) Integrable case

(b) Nonintegrable case

FIG. 3. Total nonclassicality, $\tilde{N}(t) = \sum |\tilde{p}_t(v_1, w_2, v_2, w_3)| - 1$, of the QPD, $\tilde{p}_t$, showing sensitivity to decoherence for (a) integrable and (b) scrambling systems. Comparing two timescales can reveal scrambling. The duration between the onset of nonclassicality ($\tilde{t}_* \sim 10\ \mu$s) and the first maximum ($t_m \sim 20\ \mu$s) is roughly constant across both plots. The area between t_m and the next zero (t_z) is shaded. For the integrable Hamiltonian, $t_z - t_m \sim t_m - \tilde{t}_* \sim 10\ \mu$s. For the nonintegrable Hamiltonian, $t_z - t_m$ remains an order of magnitude larger ($t_z - t_m \sim 100\ \mu$s), even with decoherence. In the decoherence-free scrambling case, $\tilde{N}(t)$ remains nonzero for at least four orders of magnitude of time longer than in the nonscrambling case.

about its first maximum. We see this lack of symmetry in the scrambling case's $\tilde{N}(t)$ in Fig. 3(b).

We see also our conjecture's role in the presence of decoherence: because of the significant differences in the scrambling-case timescales, the asymmetry persists despite the dissipation's suppression of $\tilde{N}(t)$. $F(t)$ offers no such quantitative insight: $\tilde{N}(t)$ is useful because it precisely identifies when nonclassical behavior arises and disappears.

Conclusions and outlook.—We propose that a more robust witness can be found in the nonclassical part of the QPD $\tilde{p}_t$ behind the OTOC. The total nonclassicality $\tilde{N}$ of $\tilde{p}_t$ helps distinguish integrable from scrambling Hamiltonians in the presence of decoherence. One can distinguish clearly between scrambling and nonscrambling systems by comparing two timescales of $\tilde{N}$. The duration between the birth of nonclassicality, at the time $\tilde{t}_*$, and the nonclassicality's first local maximum, at t_m, is related to the time needed by quantum information to spread throughout the system. The spreading's persistence governs the duration between t_m and the death of nonclassicality, at t_z. Nonscrambling dynamics exhibit revivals of classicality on timescales $t_m - \tilde{t}_* \approx t_z - t_m$, while scrambling dynamics take much longer. This distinction is seen clearly in the total nonclassicality $\tilde{N}(t)$. Unlike the OTOC, $\tilde{N}(t)$ is robust with respect to experimental imperfections like decoherence. Characterizing this time's scaling with system size, and checking whether the scaling can be consistent with doubly exponential expectations inspired by the Poincaré recurrence time [17,63,64], is a subject for future research.

This study of decoherence highlights two opportunities for improving the robustness and convenience of the QPD-measurement scheme in Ref. [31]. First, the weak measurements' coupling might be strengthened, along the lines in Ref. [60]. Second, the scheme in Ref. [39] might be applied to renormalize away experimental errors.

Another opportunity for future study is whether scrambling breaks symmetries in OTOC QPDs defined in terms of W and V operators other than qubit Pauli operators. An interesting choice to study next would be the Sachdev-Ye-Kitaev (SYK) model [7,65]. The SYK model consists of Majorana fermions, whose experimental realizations are being pursued assiduously [66–72]. As the SYK model scrambles maximally quickly, like black holes, it has been hoped to shed light on quantum gravity. The calculational tools available for SYK merit application to the OTOC QPD, which may shed new light on scrambling at the intersection of condensed matter and high-energy physics.

J. R. G. A. was supported by a fellowship from the Grand Challenges Initiative at Chapman University. N. Y. H. is grateful for funding from the Institute for Quantum Information and Matter, an NSF Physics Frontiers Center (NSF Grant No. PHY-1125565) with support from the Gordon and Betty Moore Foundation (GBMF-2644); a Graduate Fellowship from the Kavli Institute for Theoretical Physics, supported by the NSF under Grant No. NSF PHY-1125915; the Walter Burke Institute for Theoretical Physics at Caltech; and a Barbara Groce Graduate Fellowship. J. D. was partially supported by the Army Research Office (ARO) Grants No. W911NF-15-1-0496 and No. W911NF-1-81-0178. The authors wish to thank Paul Dieterle, Poul Jessen, Andrew Keller, Oskar Painter, and Mordecai Waegell for helpful discussions.

*Corresponding author.
gonzalezalonso@chapman.edu

[1] A. I. Larkin and Y. N. Ovchinnikov, Quasiclassical method in the theory of superconductivity, Sov. Phys. JETP **28**, 1200 (1969).
[2] A. Kitaev, Hidden correlations in the Hawking radiation and thermal noise, in *Proceedings of the Fundamental Physics Prize Symposium* (2014).
[3] S. H. Shenker and D. Stanford, Black holes and the butterfly effect, J. High Energy Phys. 03 (2014) 067.
[4] S. H. Shenker and D. Stanford, Multiple shocks, J. High Energy Phys. 12 (2014) 46.
[5] S. A. Hartnoll, Theory of universal incoherent metallic transport, Nat. Phys. **11**, 54 (2015).
[6] S. H. Shenker and D. Stanford, Stringy effects in scrambling, J. High Energy Phys. 05 (2015) 132.
[7] A. Kitaev, A simple model of quantum holography, in *Proceedings of the KITP Strings Seminar and Entanglement* (2015).
[8] D. A. Roberts, D. Stanford, and L. Susskind, Localized shocks, J. High Energy Phys. 03 (2015) 051.
[9] D. A. Roberts and D. Stanford, Diagnosing Chaos Using Four-Point Functions in Two-Dimensional Conformal Field Theory, Phys. Rev. Lett. **115**, 131603 (2015).
[10] J. Maldacena, S. H. Shenker, and D. Stanford, A bound on chaos, J. High Energy Phys. 08 (2016) 106.
[11] I. L. Aleiner, L. Faoro, and L. B. Ioffe, Microscopic model of quantum butterfly effect: Out-of-time-order correlators and traveling combustion waves, Ann. Phys. (Amsterdam) **375**, 378 (2016).
[12] M. Blake, Universal Charge Diffusion and the Butterfly Effect in Holographic Theories, Phys. Rev. Lett. **117**, 091601 (2016).
[13] M. Blake, Universal diffusion in incoherent black holes, Phys. Rev. D **94**, 086014 (2016).
[14] Y. Chen, Universal logarithmic scrambling in many body localization, arXiv:1608.02765.
[15] A. Lucas and J. Steinberg, Charge diffusion and the butterfly effect in striped holographic matter, J. High Energy Phys. 10 (2016) 143.
[16] D. A. Roberts and B. Swingle, Lieb-Robinson Bound and the Butterfly Effect in Quantum Field Theories, Phys. Rev. Lett. **117**, 091602 (2016).
[17] P. Hosur, X.-L. Qi, D. A. Roberts, and B. Yoshida, Chaos in quantum channels, J. High Energy Phys. 02 (2016) 4.
[18] S. Banerjee and E. Altman, Solvable model for a dynamical quantum phase transition from fast to slow scrambling, Phys. Rev. B **95**, 134302 (2017).

[19] R. Fan, P. Zhang, H. Shen, and H. Zhai, Out-of-time-order correlation for many-body localization, Sci. Bull. **62**, 707 (2017).

[20] Y. Gu, X.-L. Qi, and D. Stanford, Local criticality, diffusion and chaos in generalized Sachdev-Ye-Kitaev models, J. High Energy Phys. 05 (2017) 125.

[21] D. A. Roberts and B. Yoshida, Chaos and complexity by design, J. High Energy Phys. 04 (2017) 121.

[22] X. Chen and T. Zhou, Operator scrambling and quantum chaos, arXiv:1804.08655.

[23] Y. Huang, Y.-L. Zhang, and X. Chen, Out-of-time-ordered correlators in many-body localized systems, Ann. Phys. (Amsterdam) **529**, 1600318 (2017).

[24] E. Iyoda and T. Sagawa, Scrambling of quantum information in quantum many-body systems, Phys. Rev. A **97**, 042330 (2018).

[25] B. Yoshida and A. Kitaev, Efficient decoding for the Hayden-Preskill protocol, arXiv:1710.03363.

[26] C.-J. Lin and O. I. Motrunich, Out-of-time-ordered correlators in a quantum Ising chain, Phys. Rev. B **97**, 144304 (2018).

[27] S. Pappalardi, A. Russomanno, B. Žunkovič, F. Iemini, A. Silva, and R. Fazio, Scrambling and entanglement spreading in long-range spin chains, Phys. Rev. B **98**, 134303 (2018).

[28] N. Yunger Halpern, A. Bartolotta, and J. Pollack, Reconciling two notions of quantum operator disagreement: Entropic uncertainty relations and information scrambling, united through quasiprobabilities, arXiv:1806.04147.

[29] N. Y. Yao, F. Grusdt, B. Swingle, M. D. Lukin, D. M. Stamper-Kurn, J. E. Moore, and E. A. Demler, Interferometric approach to probing fast scrambling, arXiv:1607.01801.

[30] B. Swingle, G. Bentsen, M. Schleier-Smith, and P. Hayden, Measuring the scrambling of quantum information, Phys. Rev. A **94**, 040302 (2016).

[31] N. Yunger Halpern, B. Swingle, and J. Dressel, Quasiprobability behind the out-of-time-ordered correlator, Phys. Rev. A **97**, 042105 (2018).

[32] G. Zhu, M. Hafezi, and T. Grover, Measurement of many-body chaos using a quantum clock, Phys. Rev. A **94**, 062329 (2016).

[33] K. X. Wei, C. Ramanathan, and P. Cappellaro, Exploring Localization in Nuclear Spin Chains, Phys. Rev. Lett. **120**, 070501 (2018).

[34] M. Gärttner, J. G. Bohnet, A. Safavi-Naini, M. L. Wall, J. J. Bollinger, and A. M. Rey, Measuring out-of-time-order correlations and multiple quantum spectra in a trapped-ion quantum magnet, Nat. Phys. **13**, 781 (2017).

[35] J. Li, R. Fan, H. Wang, B. Ye, B. Zeng, H. Zhai, X. Peng, and J. Du, Measuring Out-of-Time-Order Correlators on a Nuclear Magnetic Resonance Quantum Simulator, Phys. Rev. X **7**, 031011 (2017).

[36] K. A. Landsman, C. Figgatt, T. Schuster, N. M. Linke, B. Yoshida, N. Y. Yao, and C. Monroe, Verified quantum information scrambling, arXiv:1806.02807.

[37] S. V. Syzranov, A. V. Gorshkov, and V. Galitski, Out-of-time-order correlators in finite open systems, Phys. Rev. B **97**, 161114 (2018).

[38] Y.-L. Zhang, Y. Huang, and X. Chen, Information scrambling in chaotic systems with dissipation, arXiv:1802.04492.

[39] B. Swingle and N. Yunger Halpern, Resilience of scrambling measurements, Phys. Rev. A **97**, 062113 (2018).

[40] B. Yoshida and N. Y. Yao, Disentangling scrambling and decoherence via quantum teleportation, arXiv:1803.10772.

[41] M. Knap, Entanglement production and information scrambling in a noisy spin system, arXiv:1806.04686.

[42] J. G. Kirkwood, Quantum statistics of almost classical assemblies, Phys. Rev. **44**, 31 (1933).

[43] P. A. M. Dirac, On the analogy between classical and quantum mechanics, Rev. Mod. Phys. **17**, 195 (1945).

[44] Y. P. Terletsky, The limiting transition from quantum to classical mechanics, J. Exp. Theor. Phys. **7**, 1290 (1937).

[45] H. Margenau and R. N. Hill, Correlation between measurements in quantum theory, Prog. Theor. Phys. **26**, 722 (1961).

[46] S. Chaturvedi, E. Ercolessi, G. Marmo, G. Morandi, N. Mukunda, and R. Simon, Wigner–Weyl correspondence in quantum mechanics for continuous and discrete systems—a dirac-inspired view, J. Phys. A **39**, 1405 (2006).

[47] N. Yunger Halpern, Jarzynski-like equality for the out-of-time-ordered correlator, Phys. Rev. A **95**, 012120 (2017).

[48] We index the W and V eigenvalues in Eq. (3) following the conventions in Refs. [31,47].

[49] G. P. Berman, F. Borgonovi, F. M. Izrailev, and V. I. Tsifrinovich, Delocalization border and onset of chaos in a model of quantum computation, Phys. Rev. E **64**, 056226 (2001).

[50] M. C. Bañuls, J. I. Cirac, and M. B. Hastings, Strong and Weak Thermalization of Infinite Nonintegrable Quantum Systems, Phys. Rev. Lett. **106**, 050405 (2011).

[51] A. Gubin and L. F. Santos, Quantum chaos: An introduction via chains of interacting spins 1/2, Am. J. Phys. **80**, 246 (2012).

[52] H. Kim and D. A. Huse, Ballistic Spreading of Entanglement in a Diffusive Nonintegrable System, Phys. Rev. Lett. **111**, 127205 (2013).

[53] Note that σ_x with an integrable Hamiltonian can simulate scrambling [26].

[54] R. Barends, J. Kelly, A. Megrant, D. Sank, E. Jeffrey, Y. Chen, Y. Yin, B. Chiaro, J. Mutus, C. Neill, P. O'Malley, P. Roushan, J. Wenner, T. C. White, A. N. Cleland, and J. M. Martinis, Coherent Josephson Qubit Suitable for Scalable Quantum Integrated Circuits, Phys. Rev. Lett. **111**, 080502 (2013).

[55] J. Koch, T. M. Yu, J. Gambetta, A. A. Houck, D. I. Schuster, J. Majer, A. Blais, M. H. Devoret, S. M. Girvin, and R. J. Schoelkopf, Charge-insensitive qubit design derived from the Cooper pair box, Phys. Rev. A **76**, 042319 (2007).

[56] Additionally, this allows us to circumvent the difficulties associated with experimentally preparing an infinite-temperature Gibbs state.

[57] I. Siddiqi (private communication).

[58] M. Khezri, J. Dressel, and A. N. Korotkov, Qubit measurement error from coupling with a detuned neighbor in circuit QED, Phys. Rev. A **92**, 052306 (2015).

[59] See Supplemental Material at http://link.aps.org/supplemental/10.1103/PhysRevLett.122.040404 for details on how to numerically simulate each OTOC-measurement protocol.

[60] J. Dressel, J. R. González Alonso, M. Waegell, and N. Yunger Halpern, Strengthening weak measurements of qubit out-of-time-order correlators, Phys. Rev. A **98**, 012132 (2018).

[61] With this definition, $\tilde{t}_*$ is close to the scrambling time t_* at which $\mathrm{Re}F(t)$ first deviates significantly from one.

[62] See Supplemental Material at http://link.aps.org/supplemental/10.1103/PhysRevLett.122.040404 for details on how the total non classicality and its time scales vary with h/J.

[63] P. Bocchieri and A. Loinger, Quantum recurrence theorem, Phys. Rev. **107**, 337 (1957).

[64] L. Campos Venuti, The recurrence time in quantum mechanics, arXiv:1509.04352.

[65] S. Sachdev and J. Ye, Gapless Spin-Fluid Ground State in a Random Quantum Heisenberg Magnet, Phys. Rev. Lett. **70**, 3339 (1993).

[66] F. Hassler, Majorana qubits, in *Quantum Information Processing. Lecture Notes of the 44th IFF Spring School 2013*, edited by D. P. DiVincenzo (Verlag des Forschungszentrums, Jülich, 2013).

[67] D. Aasen, M. Hell, R. V. Mishmash, A. Higginbotham, J. Danon, M. Leijnse, T. S. Jespersen, J. A. Folk, C. M. Marcus, K. Flensberg, and J. Alicea, Milestones Toward Majorana-Based Quantum Computing, Phys. Rev. X **6**, 031016 (2016).

[68] M. T. Deng, S. Vaitiekénas, E. Prada, P. San-Jose, J. Nygård, P. Krogstrup, R. Aguado, and C. M. Marcus, Majorana nonlocality in hybrid nanowires, Phys. Rev. B **98**, 085125 (2018).

[69] S. Vaitiekėnas, M. T. Deng, J. Nygård, P. Krogstrup, and C. M. Marcus, Effective g-Factor in Majorana Wires, Phys. Rev. Lett. **121**, 037703 (2018).

[70] R. M. Lutchyn, E. P. a. M. Bakkers, L. P. Kouwenhoven, P. Krogstrup, C. M. Marcus, and Y. Oreg, Realizing Majorana zero modes in superconductor-semiconductor heterostructures, Nat. Rev. Mater. **3**, 52 (2018).

[71] F. J. Gómez-Ruiz, J. J. Mendoza-Arenas, F. J. Rodríguez, C. Tejedor, and L. Quiroga, Universal two-time correlations, out-of-time-ordered correlators, and Leggett-Garg inequality violation by edge Majorana fermion qubits, Phys. Rev. B **97**, 235134 (2018).

[72] T. E. O'Brien, P. Rożek, and A. R. Akhmerov, Majorana-Based Fermionic Quantum Computation, Phys. Rev. Lett. **120**, 220504 (2018).